

Formation and Properties of Poly (vinyl butyral-co-vinyl alcohol-co-vinyl acetate) / Polystyrene Composites Reinforced with Graphene Oxide-Nanodiamond

Ayesha Kausar

Nanosciences and Catalysis Division, National Centre For Physics, Quaid-i-Azam University Campus, 44000, Islamabad, Pakistan

Abstract A facile and cost-effective method was used to prepare poly(vinyl butyral-co-vinyl alcohol-co-vinyl acetate) (PVBVA)/polystyrene (PS)/graphene oxide (GO) and graphene oxide-nanodiamond (GO-ND)-based nanocomposites. Formation of GO, nanodiamond functionalization of GO and nanocomposite structure were confirmed using FTIR. SEM imaging of GO, GO-ND and PVBVA/PS/GO-ND nanocomposites revealed significant results. The results revealed that nanodiamond functional GO platelets were fully incorporated into matrix. Mechanical studies depicted higher tensile strength (31.6-35.1 MPa) for PVBVA/PS/GO-ND nanocomposites compared with PVBVA/PS/GO without nanodiamonds (22.1-28.3 MPa). Thermogravimetric analysis showed higher 10% degradation temperature for nano-bifiller reinforced PVBVA/PS/GO-ND 0.1-5 as 532-554°C. Limiting oxygen index and UL 94 results depicted that PVBVA/PS/GO-ND 0.1-5 had increased non-flammability (V-1 rating) with GO-ND loading. GO-ND loading also showed electrical conductivity improvement (1.8-2.5 Scm⁻¹) relative to PVBVA/PS/GO materials (10⁻²-1.3 Scm⁻¹).

Keywords Graphene oxide-nanodiamond, Nano-bifiller, Polystyrene, Tensile strength, UL 94

1. Introduction

Polymeric nanocomposites have been primed using variety of polymer matrices (thermaoplastics, thermosetting polymers, etc.) as well as various nanofillers including carbon-based nanomaterials [1]. These nanocomposites demonstrate notable enhancement in physical characteristics such as mechanical, thermal and gas-barrier properties with the inclusion of small amount of nanofillers compared with the pristine polymers and conventional nanocomposites [2, 3]. In recent decades, range of carbon-based nanomaterials such as graphene, graphene oxide (GO) and nanodiamond (ND) have gained considerable attention owing to the outstanding physical properties. Nanodiamond has been produced and employed in different materials due to its tremendous worth in new carbon-based nanomaterial [4-6]. ND is known to have high dispersibility in polymer matrices and the resulting nanocomposites had superb physical properties, which can approach the values of single-crystal diamond [7]. Graphene, another type of nanocarbon, is two-dimensional sheet of covalently bonded sp² carbon atoms. Tremendous research has been carried out regarding graphene-based

materials due to unique structure and properties [8]. Graphene oxide (GO) is an important functionalized graphene material which have oxygen-containing functional groups on basal planes and edges of graphene [9]. These groups render the preferred characteristics for the dispersibility of the sheets in matrix. Since GO is chemically analogous to carbon nanotube and structurally akin to layered clay it has a great latent to concurrently advance not only the mechanical and barrier properties but also functional properties like electrical and thermal conductivity of polymers [10, 11]. Despite the potential advantages, the synthesis of GO-reinforced polymer nanocomposites has been challenging in obtaining well-dispersed GO sheets in polymer matrix. Several nanocomposites have been prepared with well-dispersion in polymer matrices and overcome the drawbacks of the conventional polymer/carbon-based materials. Generally, solution mixing has been used to form polymer/GO nanocomposites. Poly(methyl methacrylate) (PMMA), polyacrylic acid (PAA), polyacrylonitrile (PAN), etc. have been successfully applied in nanocomposite fabrication with GO using solution processing [12, 13]. New flame retardant approaches for polymer materials have been developed using nanocarbon additives [14-16]. In this regard many research efforts have focused on graphene, carbon nanotubes, carbon nanofibers, etc. [17-19]. However, to use of these nanoadditives as efficient flame retardants need to overcome the aggregation of nanoparticles and increase the

* Corresponding author:

asheesgreat@yahoo.com (Ayesha Kausar)

Published online at <http://journal.sapub.org/ajps>

Copyright © 2014 Scientific & Academic Publishing. All Rights Reserved

resin viscosity at high loading levels [20-23]. In this research, we have chosen a blend system of poly(vinyl butyral-co-vinyl alcohol-co-vinyl acetate) (PVBVA) and polystyrene (PS). Firstly, we have opted PVBVA as a matrix component due to the fact that its exploitation as a matrix (especially to enhance the electrical conductivity) is relatively less explored in literature. By far the most extensive use for PVBVA is in automotive and architectural applications. The polymer is also employed in coatings, binders, primers, and toners. However, the PVBVA has a tendency to crosslink which may deteriorate the final nanocomposite properties. Therefore, polystyrene was added as matrix component to improve the hybrid properties by influencing the crosslinking behavior of PVBVA. Consequently, PVBVA and PS-based nanocomposites have been developed using two type of nanocarbon structures. For this purpose, nanodiamond-functional graphene oxide (GO-ND) has been developed and both the graphene oxide and nanodiamond-functional graphene oxide were employed as nanofiller. GO-ND and ND-reinforced PVBVA/PS nanocomposites were prepared by simple casting method. The structure and properties of PVBVA/PS/GO and PVBVA/PS/GO-ND nanocomposites reinforced with GO and GO-ND were investigated using Fourier transform infrared spectroscopy (FTIR), field emission scanning electron microscopy (FESEM), thermogravimetric analysis (TGA), tensile tests, flammability and electrical conductivity.

2. Experimental Section

2.1. Materials

Poly(vinyl butyral-co-vinyl alcohol-co-vinyl acetate) (average $M_w = 120,000$) and polystyrene (average $M_w \sim 350,000$, average $M_n \sim 170,000$) were purchased from Aldrich. Detonation nanodiamond powder with size in the range of 4-5 nm was obtained from ITC, USA. Graphite was provided by Asbury Carbons, USA. Nitric acid (90%, HNO_3), sulfuric acid (98%, H_2SO_4), hydrochloric acid (37%, HCl), potassium persulfate (99 %, $K_2S_2O_8$), and phosphorus pentoxide (99%, P_2O_5) were bought from Aldrich and were used without further purification.

2.2. Instrumentation

Fourier transform infrared (FTIR) spectra were recorded using Excalibur Series FTIR Spectrometer, Model No. FTSW 300 MX manufactured by BIO-RAD. Stress-strain response of the samples (strips) with (ca. $15 \times 5.6-9.0 \times 0.45 - 0.77$ mm) dimensions was monitored according to DIN procedure 53455 using Universal Testing Machine INSTRON. Standard procedures and formulae were used to calculate stress, strain, young's modulus and toughness. The samples were cryogenically fractured in liquid nitrogen for phase morphological studies using FEI Nova 230 field emission scanning electron microscope (FE-SEM). Thermal

stability of the nanocomposites was determined by NETZSCH thermo gravimetric analyzer (TGA), model no. TG 209 F3, using 1-5 mg of the sample in Al_2O_3 crucible from upto $800^\circ C$ at a heating rate of $10^\circ C/min$ under nitrogen flow rate of 30 mL/min. LOI value was measured on samples ($100 \times 5.8 \times 3$ mm³) according to the standard oxygen index test ASTM D2863-77 using FTA IL. UL-94 test was performed ($129 \times 15.6 \times 3$ mm³) according to ASTM D635-77 for UL-94 test. Electrical conductivity was measured with four probe technique in order to avoid the contact resistance. A constant current was applied using Keithley 2400 source meter to the outer probes of the four contacts and corresponding voltage was measured with Keithley 2182 nanovoltmeter between inner probes at room temperature.

2.3. Preparation of Graphene Oxide (GO)

The graphite powder (15 g) was put into a solution of concentrated H_2SO_4 (60 mL), $K_2S_2O_8$ (7.8 g), and P_2O_5 (8.4 g) and refluxed at $80^\circ C$. After 2 h, the mixture was left to cool down to room temperature for 6 h. The mixture was then carefully diluted with 300 mL of distilled water, filtered, and washed until the pH became neutral. The product was dried at $60^\circ C$ for 48 h [24].

2.4. Synthesis of Carboxylated Nanodiamond (ND-COOH)

Nanodiamond powder (0.5g) was heated in 9:1 (v/v) mixture of concentrated H_2SO_4 and HNO_3 (30 mL) at $80^\circ C$ for 24 h. 0.1 M NaOH aqueous solution (50 mL) was added to the above mixture and was refluxed at $90^\circ C$ for 2h. Afterwards, 0.1 M HCl aqueous solution (20 mL) was added and refluxed for 2 h at $90^\circ C$. The resulting oxidized nanodiamonds were centrifuged for 6 h, filtered and washed until the pH was neutral. The product was dried at $70^\circ C$ [25].

2.5. Graphene Oxide-nanodiamond Synthesis (GO-ND)

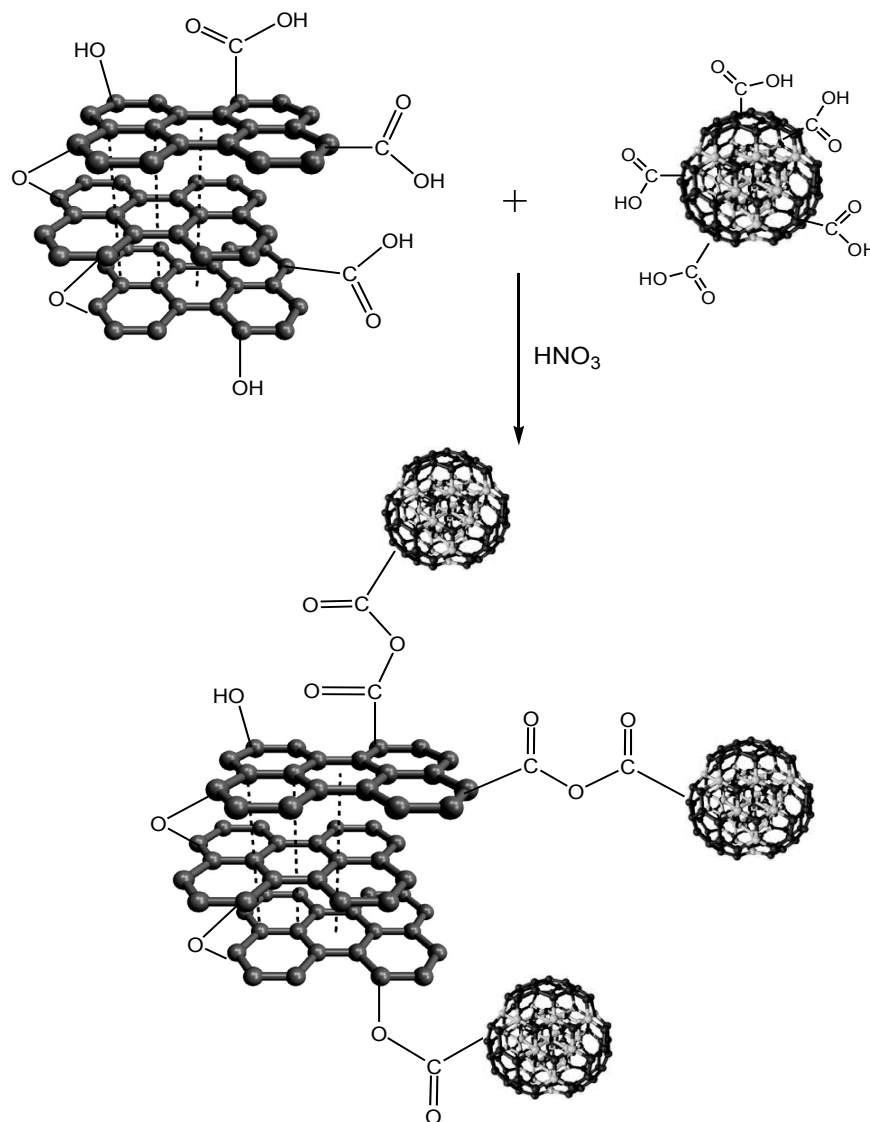
Into a 500 mL round bottom flask, GO (0.6g) and ND-COOH (0.2 g) were sonicated in 50 mL of deionized water for 6h to achieve homogeneous dispersion. Afterwards, 300 mL HNO_3 was added to the above mixture of GO and ND-COOH. The sample was again sonicated for 4 h at room temperature. After the desired time, the mixture was centrifuged for 4 h. The resulting GO-ND hybrid was washed with deionized water and filtered. Finally, the product was dried at $70^\circ C$.

2.6. Preparation of Poly(vinyl butyral-co-vinyl alcohol-co-vinyl acetate)(PVBVA)/GO-ND Nanocomposites

Typical procedure for the formation of well-dispersed PVBVA/PS/GO-ND nanocomposite includes the dispersion of GO-ND powder (0.1 g) in THF (20 mL) with sonication of 6h at room temperature. The polymer matrix was comprised of 1:1 wt. % of PVBVA: PS. Subsequently, the

solution of 1 g of PS and PVBVA was separately prepared in 10 mL THF and was added to the above GO-ND suspension. The mixture was further sonicated for 4 h to yield a stable suspension. Finally, the homogeneous PVBVA/PS/GO-ND solution was poured into a Teflon Petri

dish and kept at 60°C for film casting. Similarly, PVBVA / PS/GO-ND nanocomposite films (Fig. 1) were prepared using same procedure with loadings 0.1, 0.5, 1 and 5 wt. %, respectively, as well as one sample of pristine PVBVA/PS was also prepared.



Scheme 1. Formation of graphene oxide/nanodiamond (GO-ND) nano-bifiller

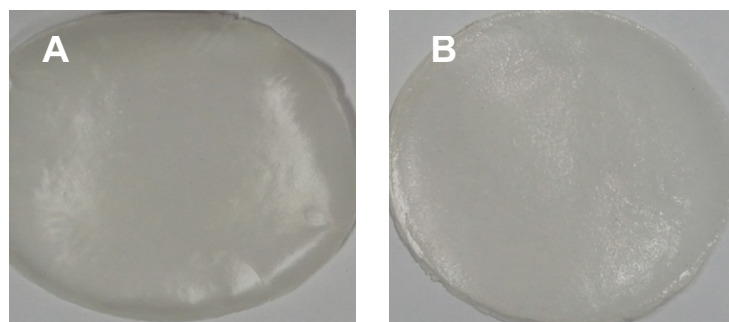


Figure 1. Films of (A) PVBVA/PS/GO 0.5; (B) PVBVA/PS/GO-ND 0.5

3. Results and Discussion

3.1. FTIR Analysis

FTIR spectra of GO, ND-COOH and GO-ND are plotted in Fig. 2.

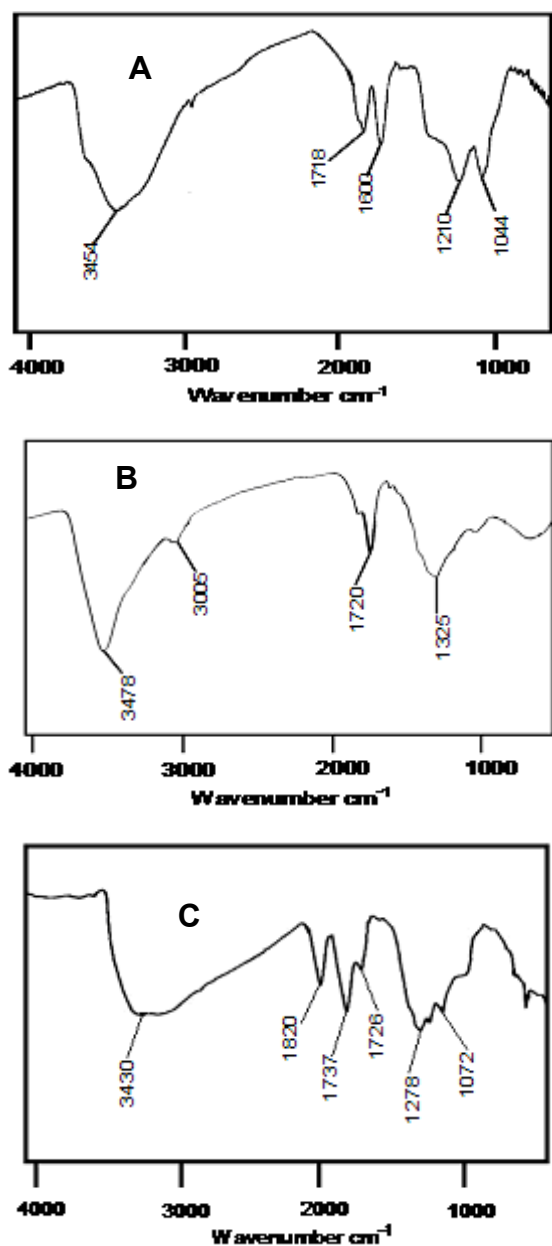


Figure 2. FTIR spectra of (A) graphene oxide; (B) carboxylated nanodiamond; and (C) GO-ND filler

The intrinsic oxygenated functionalities on GO are clearly revealed in the FTIR spectrum in Fig. 2A. The stretching vibration due to $-OH$ group from the carboxyl moiety appeared at 3454 cm^{-1} . The peak at 1718 cm^{-1} corresponds to $C=O$ of the carboxyl moiety. The un-oxidized graphite structure appeared at 1600 cm^{-1} . The $C-O$ stretching vibration of epoxide moiety appeared at 1210 cm^{-1} . The oxidized nanodiamond has the characteristic $C=O$ peaks of carboxyl moiety at 1720 cm^{-1} and $-OH$ group at 3478 cm^{-1} (Fig. 2B). The formation of GO-ND structure was also

confirmed by the FTIR (Fig. 2C). The appearance of anhydride bands at 1820 cm^{-1} and 1737 cm^{-1} and ester bands at 1726 cm^{-1} and 1278 cm^{-1} confirmed the structure. Moreover, the $-OH$ peak (3430 cm^{-1}) is significantly reduced after the GO-ND was formed. In the case of FTIR analysis of PVBVA/PS/GO-ND 0.5 (Fig. 3), all the expected vibrations appeared in the spectrum. The ester bands were found to emerge at 1717 and 1267 cm^{-1} . Moreover, the anhydride stretching vibrations were also observed at 1829 and 1777 cm^{-1} due to the filler introduced. The lowering and broadening of $-OH$ stretching vibration at 3422 cm^{-1} also confirmed the formation of polymer blend structure.

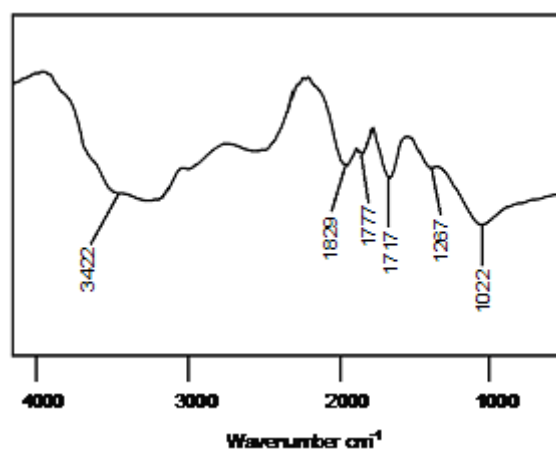


Figure 3. FTIR spectrum of PVBVA/PS/GO-ND 0.5

3.2. Morphology Investigation

The morphology of as-prepared GO, GO-ND, PVBVA/PS/GO 0.1-5 and PVBVA/PS/GO-ND 0.1-5 were investigated by field emission scanning electron microscopy. As the interaction of nano-bifillers to matrix could strengthen the interface interaction and consequently result in fine dispersion that largely determines the performance of nanocomposites. Fig. 4A shows the FESEM image of graphene oxide sheet while Fig. 4B depicts the formation of GO-ND structure. Exfoliated GO sheets embedded with nanodiamonds were visible in nano-bifiller morphology. The morphology of PVBVA/PS/GO 0.1 is given in Fig. 4C-E. The PVBVA/PS/GO-ND 0.1 shows homogeneously dispersed GO-ND in PVBVA/PS matrix and no obvious aggregation was observed in the sample. However, in Fig. 4E at higher resolution polymer coating was observed over the surface of dispersed GO-ND nano-bifiller. Moreover, no sacked structure of GO sheets was experiential due to good dispersion of GO-ND in matrix. In the case of PVBVA/PS/GO-ND nanocomposite with 0.5 wt. % filler (Fig. 5A & B), dispersion was even better relative to PVBVA/PS/GO-ND 0.1 sample. Here again the GO sheets with NDs were coated with PVBVA/PS matrix. The dispersion of 0.5 wt. % GO-NDs was better compared to other nanocomposites prepared. Fig. 5C & D represent the morphology of PVBVA/PS/GO-ND 1. Some aggregation of the nano-bifiller was visible in the matrix with 1 wt. % loading, illustrating the lack of uniform dispersion using

higher filler content. The particle size measurement of nano-filler and hybrids is given in Table 1. According to the results the least particle size was obtained for GO-ND around 30.41+1.02 nm. Whereas, the nanocomposites have increased particle size in the range of 50.01-79.10 nm due to the deposition of polymer over the nano-filler surface.

Table 1. Particle size evaluation using SEM

Sample	Particle size (nm)
GO-ND	30.41+1.02
PVBVA/PS/GO-ND 0.1	50.01+2.03
PVBVA/PS/GO-ND 0.5	73.70+2.15
PVBVA/PS/GO-ND 1	79.10+2.23

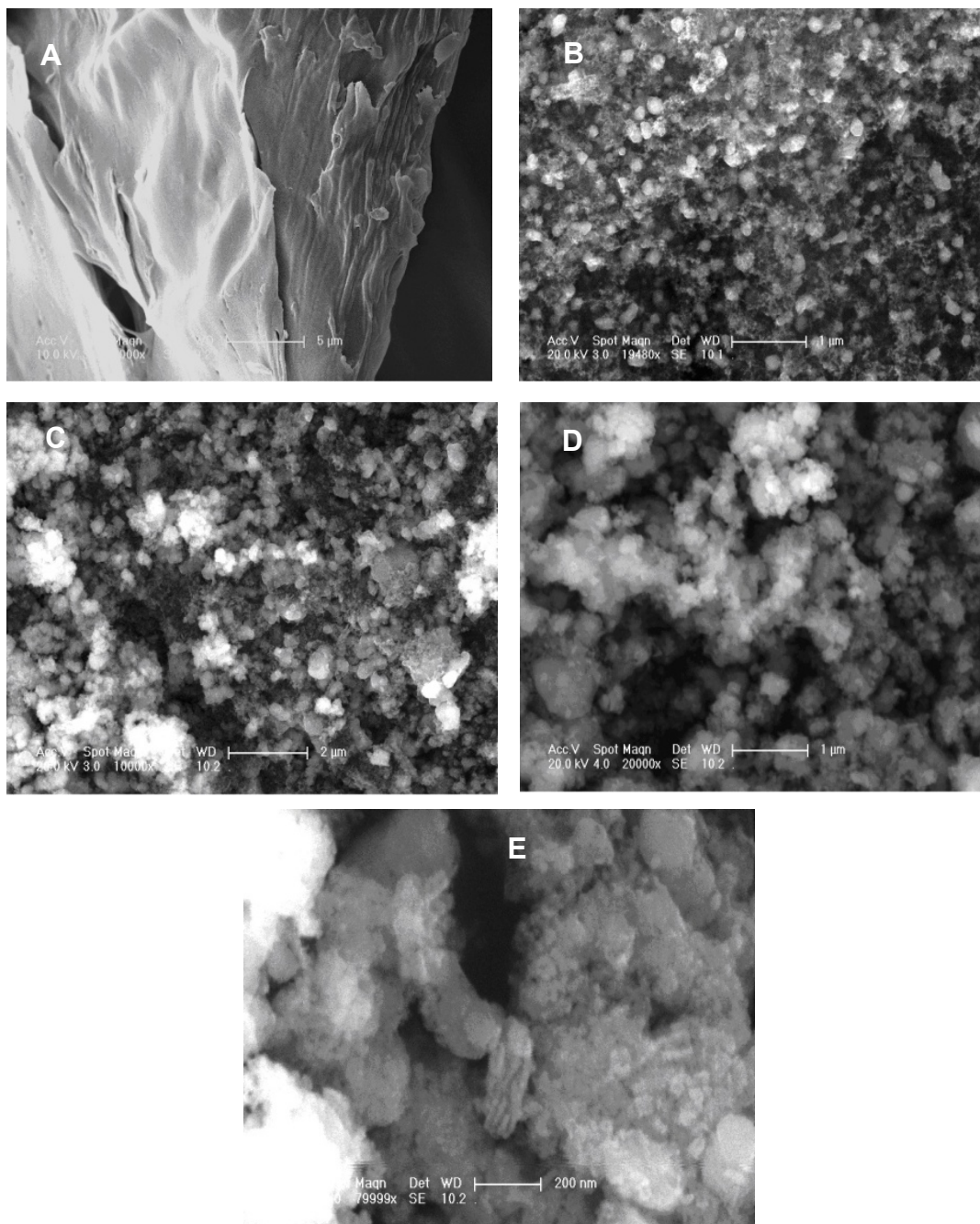


Figure 4. FESEM images of (A) GO; (B) GO-ND; (C) PVBVA/PS/GO-ND 0.1 at 2 μm; (D) PVBVA/PS/GO-ND 0.1 at 1 μm; (E) PVBVA/PS/GO-ND 0.1 at 200 nm

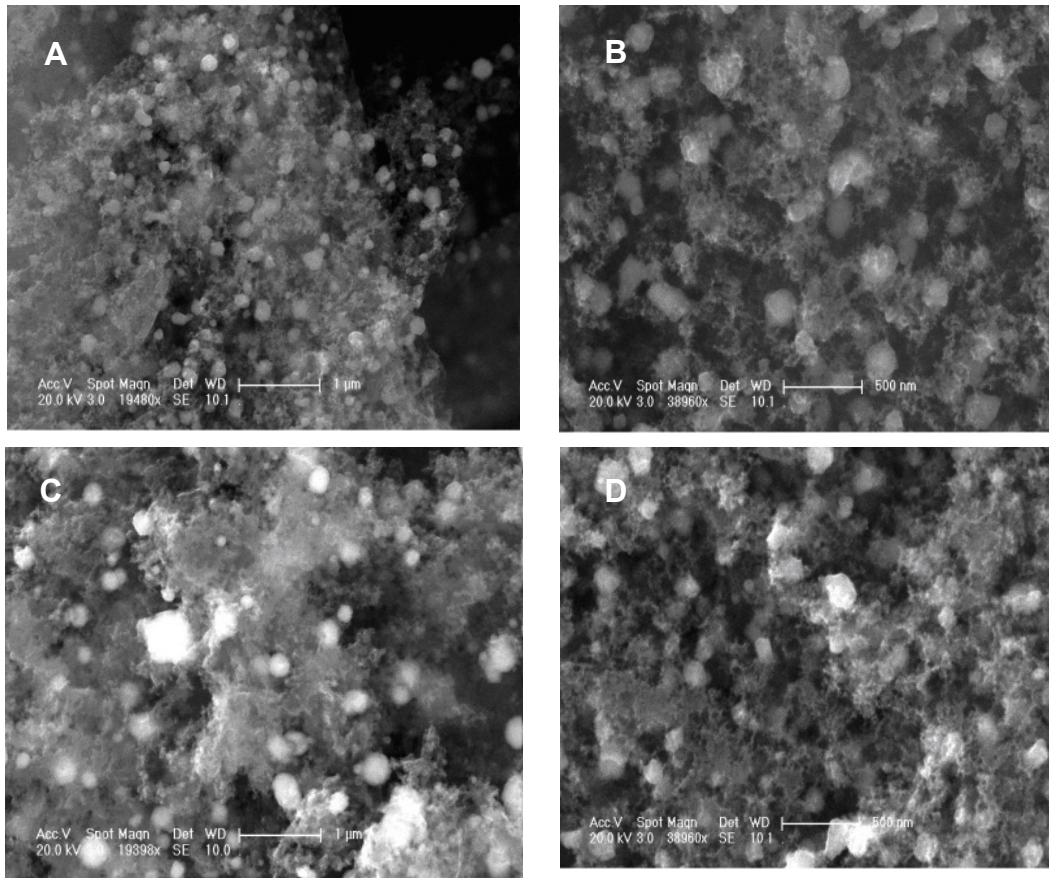


Figure 5. FESEM images of (A) PVBVA/PS/GO-ND 0.5 at 1 μm ; (B) PVBVA/PS/GO-ND 0.5 at 500 nm; (C) PVBVA/PS/GO-ND 1 at 1 μm ; (D) PVBVA/PS/GO-ND 1 at 500 nm

3.3. Tensile Studies

Tensile properties of PVBVA/PS, PVBVA/PS/GO 0.1-5 and PVBVA/PS/GO-ND 0.1-5 nanocomposites are given in Table 2. Neat PVBVA/PS demonstrated tensile strength, modulus and toughness of 21.5 MPa, 1.2 GPa and 2.5 J/m^3 . Comparing to the neat PVBVA/PS blend, PVBVA/PS/GO 0.1-5 nanocomposites showed increase in tensile strength and modulus with the graphene oxide loading. Both PVBVA/PS/GO 0.1 and PVBVA/PS/GO 0.5 nanocomposites depicted increase in tensile modulus and strength. Tensile modulus was increased up to 1.3 and 1.4 GPa in PVBVA/PS/GO 0.1 and PVBVA/PS/GO 0.5 respectively. Similarly, tensile stress was raised to 22.1 and 23.4 MPa. Toughness of the samples was also found to enhance up to 2.6 and 2.7 J/m^3 . Somewhat better results were observed for the 5 wt. % GO loaded sample, which showed an increase of 41 % in tensile modulus and 34 % in strength compared to the neat blend. Typical tensile stress-strain behavior of PVBVA/PS/GO-ND 0.1-5 nanocomposites is shown in Fig. 6. The 0.1 wt. % GO-ND nano-bifiller exhibited substantial augment in both strength and modulus up to 31.6 MPa and 3.1 GPa, compared to pure blend and GO reinforced films. The 0.5 wt. % GO-ND nanocomposite showed slight increase in properties up to 33.1 MPa and 3.2 GPa. Both of the PVBVA/PS/GO-ND

samples exhibited significantly higher toughness values (3.5 and 3.7 J/m^3) compared with neat blend and GO composites. The nanocomposites with higher GO-ND loading revealed further higher values in tensile properties. PVBVA/PS/GO-ND 1 had the tensile strength of 34.7 MPa and modulus of 3.3 GPa. PVBVA/PS/GO-ND 5 showed higher values among all the nanocomposites prepared with tensile strength of 35.1 MPa and modulus of 3.4 GPa. Toughness and strain values for this sample were also found to be higher around 3.9 J/m^3 and 3.6 %.

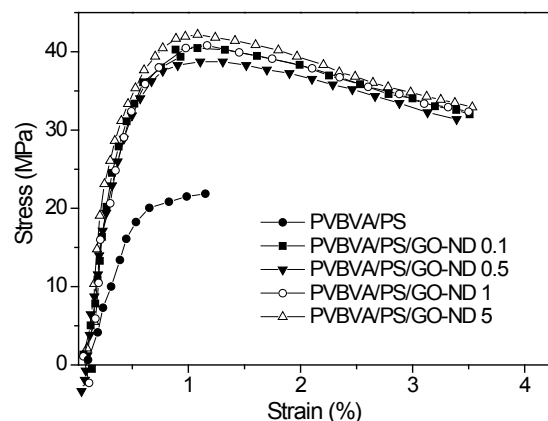
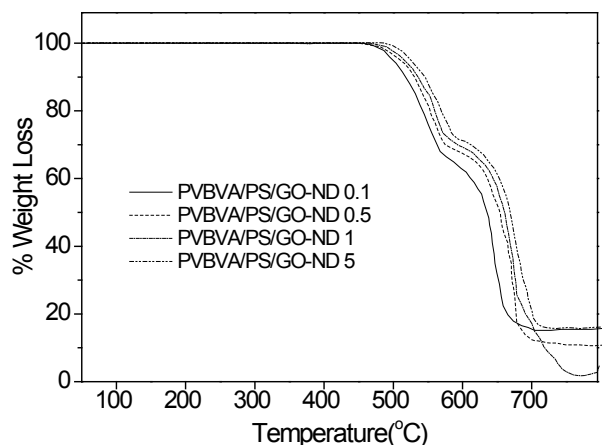


Figure 6. Stress-strain curves of PVBVA/PS/GO-ND 0.1-5 nanocomposites

Table 2. Mechanical properties of PVBVA/PS, PVBVA/PS/GO 0.1-5 and PVBVA/PS/GO-ND 0.1-5 nanocomposites

Composition	Tensile Stress (MPa) ± 0.02	Elongation at break (%) ± 0.01	Tensile Modulus (GPa) ± 0.01	Toughness (J/m ³) ± 0.05
PVBVA/PS	21.5	1.1	1.2	2.5
PVBVA/PS/GO 0.1	22.1	1.3	1.8	2.6
PVBVA/PS/GO 0.5	23.4	1.4	2.2	2.7
PVBVA/PS/GO 1	25.2	1.7	2.5	2.8
PVBVA/PS/GO 5	28.3	1.8	2.9	3.2
PVBVA/PS/GO-ND 0.1	31.6	3.3	3.1	3.5
PVBVA/PS/GO-ND 0.5	33.1	3.4	3.2	3.7
PVBVA/PS/GO-ND 1	34.7	3.5	3.3	3.8
PVBVA/PS/GO-ND 5	35.1	3.6	3.4	3.9

3.4. Thermogravimetric Analysis

**Figure 7.** TGA curves of PVBVA/PS/GO-ND 0.1-5 nanocomposites at 10 °C/min (N₂)

Thermal stability of graphene oxide-based nanocomposites is another property that may be enhanced by the incorporation of GO sheets [26]. TGA was, therefore, employed to study the thermal degradation of nanocomposites under nitrogen atmosphere. Thermal data obtained from thermogravimetric analysis of PVBVA/PS, PVBVA/PS/GO 0.1-5 and PVBVA/PS/GO-ND 0.1-5 nanocomposites are presented in Table 3. At low GO content of 0.1 wt. %, the onset degradation temperature (T_0) of the nanocomposite was improved to 454°C relative to PVBVA/PS (412°C). This was due to the homogeneously distributed and well exfoliated GO sheets which may hinder the production of thermally degraded volatile product causing the degradation. Similarly, 10 % degradation temperature (T_{10}) of PVBVA/PS/GO 0.1 was increased to 489 °C and maximum decomposition temperature (T_{max}) was found at 503 °C relative to PVBVA/PS ($T_0 = 412$ °C; $T_{10} = 449$ °C). Thermal stability of PVBVA/PS/GO 5 was found to be further increased to $T_0 = 486$ °C; $T_{10} = 522$ °C; $T_{max} = 567$ °C with 5 wt. % filler loading. Fig. 7 shows that the GO-ND sheets filled nanocomposites have significant improvement in thermal stability compared with neat PVBVA/PS and PVBVA/PS/GO 0.1-5. The thermograms

exposed two-step thermal degradation profile. Among PVBVA/PS/GO 0.1-5 materials, PVBVA/PS/GO-ND 0.1 with 0.1 wt. % nano-bifiller had T_0 of 478 °C, T_{10} of 532°C and T_{max} of 607°C. Adding up 0.5 wt. % filler in PVBVA/PS matrix further enhanced the heat constancy to T_0 , T_{10} and T_{max} of 491°C, 539°C and 612°C. PVBVA/PS/GO-ND 5 exhibited highest values of $T_0 = 510$ °C, $T_{10} = 554$ °C and $T_{max} = 632$ °C among these nanocomposites. The graphene oxide-nanodiamond nano-bifiller in fact had improved dispersion in the matrix ensuing unique morphology and enhanced thermal stability.

3.5. Flammability Tests

Table 3. Thermal analyses data of PVBVA/PS, PVBVA/PS/GO 0.1-5 and PVBVA/PS/GO-ND 0.1-5 nanocomposites

Sample	T_0 (°C)	T_{10} (°C)	T_{max} (°C)
PVBVA/PS	412	422	449
PVBVA/PS/GO 0.1	454	489	503
PVBVA/PS/GO 0.5	467	498	521
PVBVA/PS/GO 1	478	512	554
PVBVA/PS/GO 5	486	522	567
PVBVA/PS/GO-ND 0.1	478	532	607
PVBVA/PS/GO-ND 0.5	491	539	612
PVBVA/PS/GO-ND 1	500	542	627
PVBVA/PS/GO-ND 5	510	554	632

T_0 : Initial decomposition temperature

T_{10} : Temperature for 10 % weight loss

T_{max} : Maximum decomposition temperature

Table 4. LOI values and UL-94 test results of PVBVA/PS/GO 0.1-5 and PVBVA/PS/GO-ND 0.1-5 nanocomposites

Sample	LOI (%)	UL-94
PVBVA/PS/GO 0.1	25	V-0
PVBVA/PS/GO 0.5	29	V-0
PVBVA/PS/GO 1	34	V-0
PVBVA/PS/GO 5	40	V-0
PVBVA/PS/GO-ND 0.1	42	V-1
PVBVA/PS/GO-ND 0.5	45	V-1
PVBVA/PS/GO-ND 1	47	V-1
PVBVA/PS/GO-ND 5	49	V-1

LOI and UL-94 tests were used to measure the flame retardancy of PVBVA/PS/GO 0.1-5 and PVBVA/PS/GO-ND 0.1-5 nanocomposites. Effect of GO and GO-ND addition on limiting oxygen index (LOI) and UL-94 rating of neat blend and nanocomposites is illustrated in Table 4. LOI data depicted that the materials were sufficiently non-flammable. Addition of 0.1 wt. % filler in PVBVA/PS showed LOI value of 25 %. Moreover, 5 wt. % nano-bifiller in PVBVA/PS improved the LOI value to 40 %. Addition of GO-ND considerably improved the non-flammability of PVBVA/PS/GO-ND 0.1-5 nanocomposites. Maximum LOI value was obtained for PVBVA/PS/GO-ND 5 (49 %) with 5 wt. % filler loading. UL-94 test was also applied for PVBVA/PS/GO 0.1-5 and PVBVA/PS/GO-ND 0.1-5 samples. Both types of nanocomposites behaved well in UL-94 test. Graphene oxide loaded PVBVA/PS/GO 0.1-5 materials attained V-0 rating. PVBVA/PS/GO-ND 0.1-5 nanocomposites, on the other hand performed better and achieved V-1 rating in UL-94 test. Flammability results were also superior to reported graphene oxide materials [27].

3.6. Electrical Conductivity Measurement

Although the reported electrical conductivity of graphene oxide has been known much lower than graphene, the graphene oxide and nanodiamond nano-bifiller was expected to form conducting network supporting the increased electrical conductivity. The electrical conductivity values for PVBVA/PS/GO 0.1-5 and PVBVA/PS/GO-ND 0.1-5 nanocomposites are listed in Table 5. The electrical conductivity of PVBVA/PS/GO 0.1-5 nanocomposite films was found in the range 10^{-2} - 1.3 Scm^{-1} . On the other hand, PVBVA/PS/GO-ND 0.1-5 nanocomposites had higher values in the electrical conductivity 1.8 - 2.5 Scm^{-1} . Generally speaking, rapid increase in the electrical conductivity of GO-ND-based nanocomposites implies the formation of a conducting network throughout the insulating polymer matrix [28, 29]. However, PVBVA/PS/GO 0.1-5 nanocomposites were still sufficiently electrically conductive, which may also be attributed to the network between PVBVA/PS matrices and GO generating some conductive pathways in the nanocomposites.

Table 5. Conductivity measurement of nanocomposites

Sample	Conductivity (S cm^{-1})
PVBVA/PS	10^{-8}
PVBVA/PS/GO 0.1	10^{-2}
PVBVA/PS/GO 0.5	10^{-1}
PVBVA/PS/GO 1	1.2
PVBVA/PS/GO 5	1.3
PVBVA/PS/GO-ND 0.1	1.8
PVBVA/PS/GO-ND 0.5	1.9
PVBVA/PS/GO-ND 1	2.1
PVBVA/PS/GO-ND 5	2.5

4. Conclusions

Graphene oxide was directly functionalized with nanodiamonds to form nano-bifiller. The GO and GO-ND were afterwards introduced into PVBVA/PS blend structure to obtain PVBVA/PS/GO and PVBVA/PS/GO-ND nanocomposites. GO-ND sheets were dispersed well in matrices without any reaggregation, and they were partly covered with polymers. The nanocomposites exhibited a significant improvement in mechanical property and thermal stability at GO and GO-ND loading level of 0.1-5 wt. %. As the functionalization of GO with ND affords a facile and cost-effective way to prepare nanodiamond decorated graphene oxide and PVBVA / PS-based nanocomposites with high performance. Nano-dispersion of functional graphene oxide also resulted in non-flammable nanocomposite with enhanced electrical, thermal, mechanical and morphological properties. One of the fine achievements was the accomplishment of LOI values between 42-49 % and V-1 rating of PVBVA/PS / GO-ND 0.1-5. Moreover nanodiamond in combination with GO revealed better flame retardant effects. Conductivity measurements performed highlighted that the nano-diamond filler enhanced the conductive properties. Novel materials can be engineered into thermal spray coatings to provide different degrees of electrical conductivity.

REFERENCES

- [1] Hu, K., Kulkarni, D. D., Choi, I., Tsukruk, V. V., 2014, Graphene-polymer nanocomposites for structural and functional applications. *Prog. Polym. Sci.*, DOI: 10.1016/j.progpolymsci.2014.03.001.
- [2] Morimune, S., Kotera, M., Nishino, T., 2010, Stress transfer of poly (vinyl alcohol)/montmorillonite nanocomposite using X-ray diffraction. *J. Adhes. Soc. Japan.*, 46(9), 320-325.
- [3] Wei, C., Srivastava, D., Cho, K., 2002, Thermal Expansion and Diffusion Coefficients of Carbon Nanotube- Polymer Composites. *Nano Lett.*, 2(6), 647-650.
- [4] Greiner R., Phillips D. S., Johnson J. D., Volk A. F., 1988, Diamonds in detonation soot. *Nature*, 333(), 440-442.
- [5] Lam, R., Chen, M., Pierstorff, E., Huang, H., Osawa, E., Ho, D., 2008, Nanodiamond Embedded Microfilm Devices for Localized Chemotherapeutic Elution. *ACS Nano.*, 2(10), 2095-2102.
- [6] Behler, K. D., Stravato, A., Mochalin, V., Korneva, G., Yushin, G., Gogotsi, Y., 2009, Nanodiamond-polymer composite fibers and coatings. *ACS Nano.*, 3(2), 363-369.
- [7] Morimune, S., Kotera, M., Nishino, T., Hata, K., Goto, K., 2011, Poly (vinyl alcohol) Nanocomposites with Nanodiamond. *Macromolecules*, DOI: 10.1021/ma200176r.
- [8] Novoselov, K. S., Geim, A. K., Morozov, S. V., Jiang, D.,

- Zhang, Y., Dubonos, S. V., Grigorieva, I. V., Firsov, A. A., 2004, Electric Field Effect in Atomically Thin Carbon Films. *Science*, 306(5696), 666-669.
- [9] Kim H., Abdala A., Macosko C., 2010, Graphene/Polymer Nanocomposites. *Macromolecules*, 43(16), 6515-6530.
- [10] Geim, A. K., Novoselov, K. S., 2007, The rise of graphene. *Nat. Mater.*, 6(3), 183-191.
- [11] Sun, X., Liu, Z., Welscher, K., Robinson, J. T., Goodwin, A., Zaric, S., Dai, H., 2008, Nano-Graphene Oxide for Cellular Imaging and Drug Delivery. *Nano. Res*, 1(3), 203-212.
- [12] Ramanathan, T., Abdala, A. A., Stankovich, S., Dikin, D. A., Herrera-alonso, M., Piner, R. D., Adamson, D. H., Schniepp, H. C., Chen, X., Ruoff, R. S., Nguyen, S. T., Aksay, I. A., Prudhomme, R. K., Brinson, L. C., 2008, *Nat. Nanotechnol.*, 3(6), 327-331.
- [13] Kim, H., Macosko, C. W., 2008, Morphology and Properties of Polyester/Exfoliated Graphite Nanocomposites. *Macromolecules*, 41(9), 3317-3327.
- [14] Isitman, N. A., Dogan, M., Bayramli, E., Kaynak, C., 2012, The role of nanoparticle geometry in flame retardancy of polylactide nanocomposites containing aluminium phosphinate. *Polym. Degrad. Stab.*, 97(8), 1285-1296.
- [15] Isitman, N. A., Kaynak, C., 2010, Nanoclay and carbon nanotubes as potential synergists of an organophosphorus flame-retardant in poly (methylmethacrylate). *Polym. Degrad. Stab.*, 95(9), 1523-1532.
- [16] Dong W., Zhang X., Liu Y., Liu Y., Wang Q., Gui H., Gao J., Song Z., Lai J., Huang F., Qiao J., 2006, Flame retardant nanocomposites of polyamide 6/clay/silicone rubber with high toughness and good flowability. *Polymer*, 47(19), 6874-6879.
- [17] Kashiwagi T., Du F., Winey K. I., Groth K. M., Shields J. R., Bellayer S. P., Kim H., Douglas J. F., 2005, Flammability properties of polymer nanocomposites with single-walled carbon nanotubes: effects of nanotube dispersion and concentration. *Polymer*, 46(2), 471-481.
- [18] Kashiwagi T., Du F., Douglas J. F., Winey K. I., Harris Jr R. H., Shields J. R., 2005, Nanoparticle networks reduce the flammability of polymer nanocomposites. *Nat. Mater.*, 4(12), 928-933.
- [19] Tang, Y., Zhuge, J., Gou, J., Chen, R., Ibeh, C., Hu Y., 2011, Morphology, thermal stability, and flammability of polymer matrix composites coated with hybrid nanopapers. *Polym. Adv. Technol.*, 22(10), 1403-1413.
- [20] Lao, S. C., Yong, W., Nguyen, K., Moon, T. J., Koo, J. H., Pilato, L., Wissler, G., 2010, Flame-retardant polyamide 11 and 12 nanocomposites: processing, morphology, and mechanical properties. *J. Compos. Mater.*, 44(25), 2933-2951.
- [21] Song P. A., Liu L. N., Fu S. Y., 2013, Striking multiple synergies created by combining reduced graphene oxides and carbon nanotubes for polymer nanocomposites. *Nanotechnology*, 24(12), 25704-25704.
- [22] Liao S. H., Liu P., Hsiao M., Teng C. -C., Wang C. -A., Ger M. -D., Chiang C. -L. 2012, One-step reduction and functionalization of graphene oxide with phosphorus-based compound to produce flame-retardant epoxy nanocomposite. *Indus. Eng. Chem. Res.*, 51(12), 4573-4581.
- [23] Chapple, S., Anandjiwala, R., 2010, Flammability of natural fiberreinforced composites and strategies for fire retardancy: a review. *J. Thermoplast. Compos. Mater.*, 23(6), 871-893.
- [24] Zhang, L. L., Zhao, S., Tian, X. N., Zhao, X. S., 2010, Layered graphene oxide nanostructures with sandwiched conducting polymers as supercapacitor electrodes. *Langmuir*, 26(22), 17624-17628.
- [25] Sun, Y., Wu, Q., Xu, Y., Bai, H., Li, C., Shi, G., 2011, Highly conductive and flexible mesoporous graphitic films prepared by graphitizing the composites of graphene oxide and nanodiamond. *J. Mater. Chem.*, 21(20), 7154-7160.
- [26] Feng, L., Guan, G., Li, C., Zhang, D., Xiao, Y., Zheng, L., Zhu, W., 2013, In-situ synthesis of poly (methylmethacrylate)/ graphene oxide nanocomposites using thermal initiated and graphene oxide-initiated polymerization. *J. Macromol. Sci. A Pure Appl. Chem.*, 50(7), 720-727.
- [27] Liao S., Liu P., Hsiao M., 2012, One-step reduction and functionalization of graphene oxide with phosphorus-based compound to produce flame-retardant epoxy nanocomposite. *Indus. Eng. Chem. Res.*, 51(12), 4573-4581.
- [28] Lee, S. H., Cho, E., Jeon, S. H., Youn, J. R., 2007, Rheological and electrical properties of polypropylene composites containing functionalized multi-walled carbon nanotubes and compatibilizers. *Carbon*, 45(14), 2810-2822.
- [29] Stankovich, S., Dikin, D. A., Dommett, G. H. B., Kohlhaas, K. M., Zimney, E. J., Stach, E. A., Piner, R. D., Nguyen, S. T., Ruoff, R. S., 2006, Graphene-based composite materials. *Nature*, 442(7100), 282-286.